Systematic study of odd-even staggering in elemental fragmentation cross sections for N=Z nuclei from ^{36}Ar to ^{28}Si at ~ 300 MeV/nucleon*

Yu-Nan Song (宋雨楠)[1,2,3] Yong Zheng (郑勇)[1†] Guang-Shuai Li (李光帅)[4] Bao-Hua Sun (孙保华)[4‡]
Jun Su (苏军)[5] Ge Guo (郭戈)[4] Kai-Long Wang (王凯龙)[1] Jun-Yao Xu (徐俊瑶)[4] Xiao-Dong Xu (徐晓栋)[1]
Ji-Chao Zhang (张寂潮)[4] Meng Wang (王猛)[1§] Xiu-Lin Wei (魏秀琳)[4] Yong Cao (曹勇)[4]
Bing-Shui Gao (高丙水)[1] Yun Qin (秦赟)[4] Lu-Ping Wan (万鲁平)[4] Chang-Jian Wang (王长建)[4]
Xin-Xu Wang (王昕旭)[4] Wen-Wen Zhang (张文文)[4] Xiao-Bin Zhang (张小彬)[4] Zi-Cheng Zhou (周子铖)[4]

[1]Institute of Modern Physics, Chinese Academy of Sciences, Lanzhou 730000, China
[2]School of Nuclear Science and Technology, Lanzhou University, Lanzhou 730000, China
[3]School of Nuclear Science and Technology, University of Chinese Academy of Sciences, Beijing 100049, China
[4]School of Physics, Beihang University, Beijing 100191, China
[5]Sino-French Institute of Nuclear Engineering and Technology, Sun Yat-sen University, Zhuhai 519082, China

Abstract: Elemental fragmentation cross sections (EFCSs) of the $N = Z$ nuclei ^{36}Ar, ^{34}Cl, ^{32}S, ^{30}P, and ^{28}Si on a carbon target were measured at approximately 300 MeV/nucleon using the RIBLL2 fragment separator at HIRFL. Among these, the cross sections for ^{34}Cl and ^{30}P are reported here for the first time, providing new data and extending EFCS measurements along the $N = Z$ chain. The measured cross sections exhibit significant odd-even staggering as a function of the charge change ΔZ. The experimental results are compared with several empirical parametrizations, including Cummings, EPAX3, and FRACS, as well as with the isospin-dependent quantum molecular dynamics model (IQMD) coupled to the statistical decay code GEMINI. The IQMD+GEMINI calculations reproduce the experimental cross sections with an accuracy of approximately 7% and reasonably reproduce the observed odd-even staggering. Consistent with previous studies, comparisons of model predictions at different reaction stages demonstrate that the odd-even staggering in EFCSs predominantly originates from the de-excitation of excited primary fragments. These results further establish the robustness of this interpretation by extending its validity to the $N = Z$ region.

Keywords: elemental fragmentation cross section, IQMD+GEMINI model, odd-even staggering

DOI: 10.1088/1674-1137/ae5d27 **CSTR:** 32044.14.ChinesePhysicsC.50061001

I. INTRODUCTION

The advent of relativistic radioactive ion beam facilities worldwide, such as FRS at GSI [1], CSR-RIBLL2 at IMP [2, 3] and BigRIPS at RIKEN [4], has enabled systematic investigations of the interaction properties for nuclei ranging from the valley of stability to the drip lines. The elemental fragmentation cross section (EFCS), defined as the probability that a projectile nucleus loses a specific number of protons after colliding with a target nucleus, is a fundamental observable in nucleus-nucleus collisions. The study of EFCSs plays an important role in advancing our understanding about reaction mechanisms and the nuclear structure [5−8].

Experimentally, EFCS data measured at relativistic energies exhibit a pronounced odd-even staggering, which means an enhanced production of even-Z fragments relative to the neighboring odd-Z ones [5, 9−14]. Such staggering effect has been observed in different projectile-target combinations and is found to correlate with the isospin ($T_Z = Z - A/2$) of the nuclei. The effect is seen to be relatively strong for neutron-deficient beams and gradually weakens with increasing T_Z of the projectile [15, 16].

Experimental data on EFCS also contributed to the development of theoretical modes. Several empirical parametrizations have been proposed to predict charge and isotopic distributions in relativistic heavy-ion colli-

Received 26 March 2026; Accepted 8 April 2026; Accepted manuscript online 9 April 2026
* The work is supported by the National Natural Science Foundation of China (12325506, U1832211)
† E-mail: zhengyong@impcas.ac.cn
‡ E-mail: bhsun@buaa.edu.cn
§ E-mail: wangm@impcas.ac.cn

sions, including different versions of the Cummings parametrization [17, 18] and EPAX [19–21] models. On the other hand, quantum molecular dynamics approaches, such as the original IQMD [22], as well as its improved versions ImQMD [23] and RQMD [24], have been developed to calculate the fragmentation cross sections. Although these models can give reasonable predictions for EFCSs, they generally fail to reproduce the odd-even staggering observed in the experimental data.

The prevailing interpretation of the odd-even staggering observed in fragmentation cross sections is that it originates from the structure effects in excited nuclei, such as pairing, shell effects, and nuclear level density [5, 7]. These effects may appear in the reaction mechanism when part of the reaction proceeds through low excitation energies. Indeed, in the previous work, Li *et al*. employed the hybrid IQMD+GEMINI model [6], which couples the IQMD framework [22] with the statistical decay model GEMINI [25], to successfully reproduce the observed odd-even staggering in the EFCSs obtained from the fragmentation reactions of ^{28}Si on a carbon target at 218 MeV/nucleon [14]. Comparison between the experimental EFCS data and the calculations indicates that this staggering emerges during the statistical de-excitation of the highly excited prefragments, rather than from the initial dynamical stage of the reaction. Wei *et al*. applied the same model to $^{32-38}$S [16], the results also showed good agreement with the experimental data. They also found that the odd-even staggering in the EFCSs exhibits a universal trend with the projectile nuclear T_Z.

Despite progress in both theoretical and experimental studies, the formation mechanism of the odd-even staggering effect remains not fully understood, which calls for more systematic measurements of EFCSs. This work aims to provide a set of data that enables a systematic investigation of the effect along the chain of $N = Z$ projectile nuclei, where the staggering is known to be relatively pronounced.

We report the measurement of EFCSs for the $N = Z$ nuclei ^{36}Ar, ^{34}Cl, ^{32}S, ^{30}P, and ^{28}Si on a carbon target. The incident energies of these projectiles are approximately 300 MeV/nucleon, which is higher than that of our previous works [14, 16, 26], for which the incident energies were around 220 MeV/nucleon. Among these, the cross sections for ^{34}Cl and ^{30}P are reported for the first time. This paper is organized as follows. In Sec. II, we describe the experimental configuration and the data analysis procedure. The experimental results and theoretical calculations are presented in Sec. III, with a focus on the odd-even staggering observed in the EFCSs and the systematics along the chain of $N = Z$ projectile nuclei. Finally, a summary is provided in Sec. IV.

II. EXPERIMENT AND DATA ANALYSIS

The experiment was conducted at the second Radioactive Ion Beam Line in Lanzhou (RIBLL2) [2, 3], located in the Heavy Ion Research Facility in Lanzhou [27]. A schematic drawing of the RIBLL2 facility is presented in Fig. 1, with the detector setup for the present measurement at the F4 focal plane shown inset. A primary ^{40}Ar beam, after being accelerated to 400 MeV/nucleon at the main cooling storage ring, impinged upon a 10-mm beryllium target located at the F0 focal plane to produce secondary radioactive beams. These secondary beams were subsequently separated and transported by the RIBLL2 beamline towards the F4 focal plane, where the reaction target and main detector system were placed. Two multi-wire proportional chambers (MWPC1 and MWPC2 [28]) were installed at F2 and F3, respectively, in order to monitor the position of the in-flight fragments.

A carbon reaction target (10 mm in thickness) was placed at the middle of the F4 platform. The thickness variation of the reaction target was measured to be less than 0.1%, contributed as part of the systematic uncertainty. On either side of the reaction target, two sets of ionization detectors were installed. Each set consisted of a pair of multi-wire drift chambers (MWDC) and a multiple sampling ionization chamber (MUSIC) [29] placed between them. The MWDCs with a position resolution of 0.1 mm (σ) [30], were used to reconstruct the track of the fragments, thereby ensuring the acceptance of the whole detector system.

The particle identification of the secondary beams was successfully performed by the Bρ-ΔE-time-of-flight ($B\rho - \Delta E - TOF$) method. The TOF was measured by two fast-timing plastic scintillators, namely TOF-Start and TOF-Stop, each with a thickness of 1 mm. The TOF-Start detector [31], with a sensitive area of 100 mm×100 mm, was placed at the F1 focal plane, downstream a pair of slits. The TOF-Stop detector [32, 33] featuring a sensitive area of 50 mm×50 mm was installed at the front end of F4 platform. Such two detectors achieved a TOF resol-

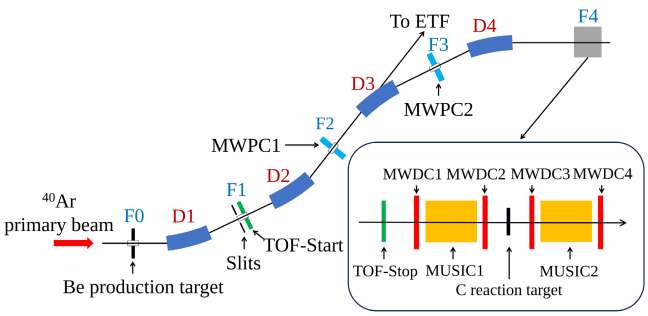

Fig. 1. (color online) Schematic diagram of the RIBLL2 separator. F0–F4 denote the focal planes along the beamline, and D1–D4 denote the dipole magnets. The inset shows the detector setup at F4 (not to scale).

ution of 75 ps (σ). The energy losses (ΔE) of fragments incident and outgoing the reaction target were measured separately by MUSIC1 and MUSIC2, respectively. We also performed an additional experimental setting with the reaction target removed for comparative purposes.

Fig. 2(a) shows the particle identification spectrum of the incident fragments. Incorrect events from abnormal detector responses have been excluded beforehand, and TOF was corrected to get rid of position dependence. The data analysis procedure for the incident fragments was described in-depth in Ref. [34]. The central column of plots correspond to events from $N = Z$ nuclei. We apply ellipse-like gates to isolate the $N = Z$ beams for further analysis, which are shown by dashed curves. Possible contamination from neighboring nuclei is estimated to be generally around 0.01%, and is included in the systematic uncertainty evaluation.

Fig. 2(b)-(f) displays the ΔE distribution of outgoing fragments originating from the incident $N = Z$ beams. Peaks corresponding to fragments with charge numbers $Z > 7$ can be clearly figured out from the spectrum, while the lighter fragments lie beyond the sensitive range of MUSIC2, consequently, the spectral resolution for such range is insufficient for precise analysis. Here we mainly focus on the fragments with $Z > 7$. To quantify the yield of each Z, multiple-Gaussian functions were fitted to each spectrum. The reduced chi-square values of these fits are generally below 1.12, indicating a good description of the spectrum.

III. RESULT AND DISCUSSION

The EFCS for a nuclide losing ΔZ protons after reacting with the target nucleus is generally calculated as:

$$\sigma_{\Delta Z} = \frac{1}{t}\left(\frac{N_F}{N_{\rm in}} - \frac{N_F^0}{N_{\rm in}^0}\right), \tag{1}$$

where $N_{\rm in}$ and N_F denote the numbers of incident projectiles with $Z = Z_P$ and outgoing fragments with $Z = Z_P - \Delta Z$, respectively, whereas $N_{\rm in}^0$ and N_f^0 are the corresponding quantities measured without the reaction target. Here, t denotes the number of target nuclei per unit area.

According to Ref. [14], for a relatively thick reaction target such as the one used in this experiment, the target thickness and secondary reactions of incident fragments within the target can lead to imprecise EFCS results, especially for larger charge changes ΔZ. Therefore, Eq. 1 becomes unreliable. When secondary reactions are taken into account, their contribution is negligible for small ΔZ or a thin target, and the EFCS can be calculated as:

$$\sigma_{\Delta Z} = \left(\frac{N_F}{N_{\rm in}} - \frac{N_F^0}{N_{\rm in}^0}\right)\frac{\sigma_R^P}{1-\exp(-\sigma_R^P t)}, \tag{2}$$

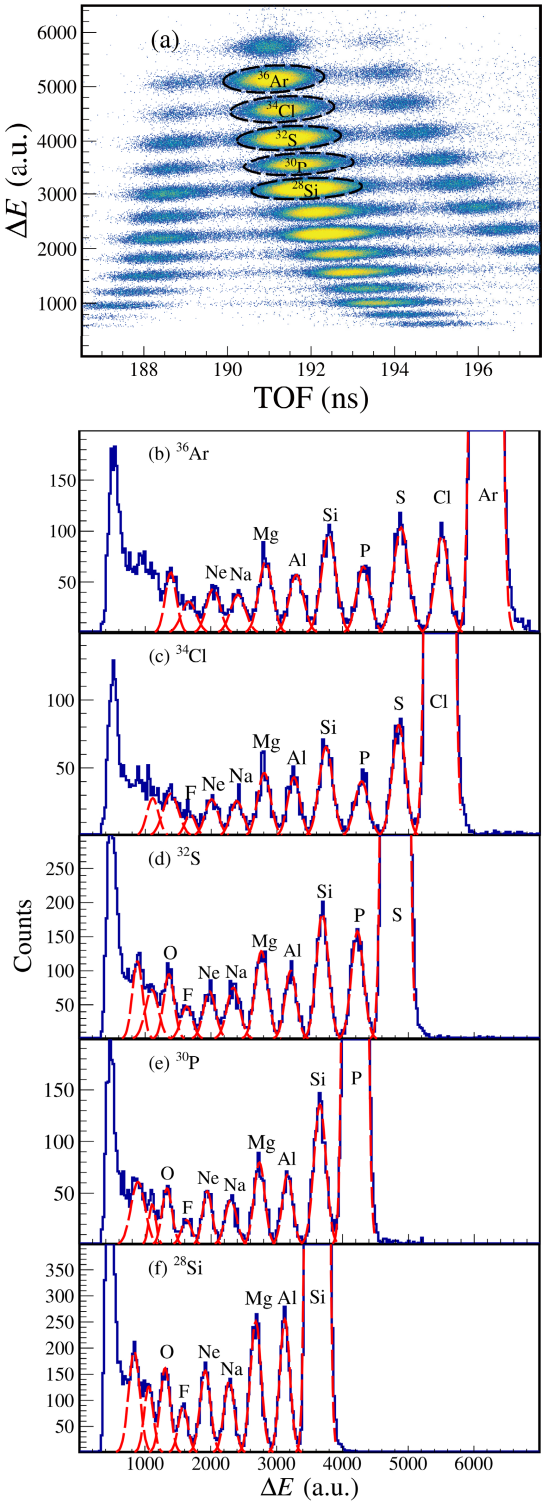

Fig. 2. (color online) (a) Particle-identification spectrum of the cocktail beams produced by ^{40}Ar + ^{9}Be at 400 MeV/nucleon. The dashed ellipses indicate the gates used to select the ^{36}Ar, ^{34}Cl, ^{32}S, ^{30}P, and ^{28}Si ions. (b)-(f) ΔE distributions of fragments produced by the aforementioned projectiles impinging on a carbon target. The dashed curves show the multi-Gaussian functions used to fit the experimental distributions.

where σ_R^P denotes the reaction cross section of the projectile on the target. In the current analysis, the σ_R^P values for $N = Z$ nuclei were calculated using a zero-range optical-limit Glauber model with an energy-dependent phenomenological correction factor, as described in Ref. [35].

For large ΔZ values and/or thick targets, secondary reactions become more significant; thus, the following equation is used:

$$\sigma_{\Delta Z} = \left(\frac{N_F}{N_{\rm in}} - \frac{N_F^0}{N_{\rm in}^0}\right) \frac{\sigma_{\rm CC}^F - \sigma_R^p}{\exp(-\sigma_R^P t) - \exp(-\sigma_{\rm CC}^F t)}, \qquad (3)$$

where $\sigma_{\rm CC}^F$ is the total charge-changing cross section for the assumed intermediate fragment F on the target. $\sigma_{\rm CC}^F$ is calculated within the same framework as σ_R^P. Although the treatment relies on a specific assumption, a 10% variation in $\sigma_{\rm CC}^F$ changes the resulting EFCS by only 0.4%.

The EFCSs ($\sigma_{\Delta Z}$) of the $N = Z$ projectiles ^{36}Ar, ^{34}Cl, ^{32}S, ^{30}P and ^{28}Si measured in this work are presented in Fig. 3 as a function of ΔZ. The error bars represent the combination of statistical and systematic errors. We apply Eq. (2) for $\Delta Z = 1-2$, yielding results that are systematically higher than those from Eq. (1) by approximately 6%. For $\Delta Z > 4$, Eq. (3) is used, resulting in an additional 5% increase compared to the results obtained using Eq. (2). For $\Delta Z = 3-4$, we adopt the average of the results from Eq. (1) and Eq. (3). The deviation between the two equations is included as part of the systematic uncertainty.

We also plot previous experimental data at similar incident energies in Fig. 3 for comparison. The data for ^{36}Ar and ^{28}Si from this work show good agreement with those measured by Sawahata *et al.* [13], and with the ^{28}Si data at 344 MeV/nucleon measured by Zeitlin *et al.* [12]. Ref. [12] also measured the EFCSs of ^{28}Si at 266 MeV/nucleon; however, despite the incident energy being very close to that in Ref. [13], a systematic deviation exists between the two data sets. For ^{32}S, our data are generally lower than those from Wei *et al.* [16], and a similar discrepancy is observed when comparing the ^{28}Si data with the work of Li *et al.* [14]. The deviations between the present data and those from the above two works can be explained by the energy dependence of the EFCS reported in Ref. [14].

Calculations using the IQMD+GEMINI model, along with other models, are shown in Fig. 3. The experimental data of the five $N = Z$ nuclei exhibit two features: the EFCSs systematically decrease as more protons are removed from the projectile, and a clear odd-even staggering is observed for all projectiles; that is, the cross sections for even-Z final fragments are enhanced relative to those of the neighboring odd-Z ones. The IQMD+GEMINI calculations successfully reproduce both features and the experimental data with an overall accuracy of about 7%.

In contrast, the empirical parametrizations of Cummings and EPAX3 fail to reproduce the odd-even staggering, as both show a monotonically decreasing trend with increasing ΔZ. The FRACS empirical parametrization [36], which introduces energy dependence and an additional odd-even term based on EPAX, generally follows the experimental trend for $N = Z$ projectiles, reproducing the experimental data with an accuracy of approx-

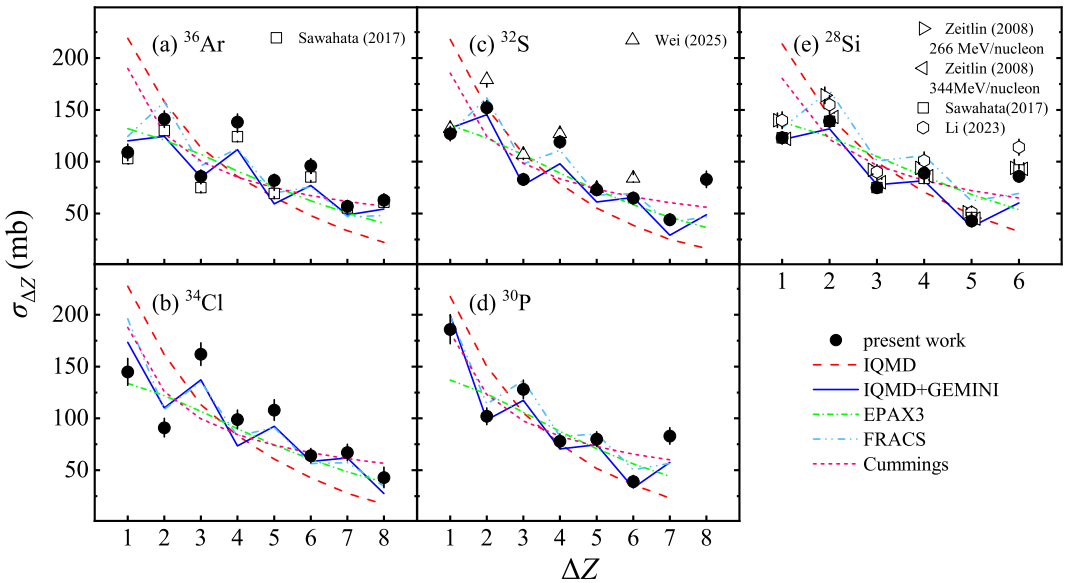

Fig. 3. (color online) Elemental fragmentation cross sections for the $N = Z$ nuclei ^{36}Ar, ^{34}Cl, ^{32}S, ^{30}P, and ^{28}Si plotted as a function of ΔZ. Experimental data from the present work and from previous studies are shown as filled circles and open symbols, respectively. Model predictions are indicated by different line styles. Data points with similar values are slightly offset for clarity.

imately 10%, which is slightly lower than that of IQMD+GEMINI. However, FRACS systematically overestimates the EFCSs for ^{28}Si by 10%−40%.

It should be emphasized that the IQMD calculation alone describes the formation of highly excited prefragments at the end of the dynamical stage, rather than the final cold fragments measured in the experiment. In the IQMD framework, each nucleon is propagated under the combined action of the self-consistent mean field and stochastic nucleon-nucleon collisions [37]. Prefragments are identified by the minimum spanning tree algorithm at a finite switching time of the order of 10^2 fm/c. These prefragments are therefore intermediate states of the reaction rather than the final observed fragments. As shown in Fig. 3, the IQMD calculation yields a monotonic decrease in cross sections with increasing ΔZ, failing to reproduce the significant odd-even staggering observed in the experimental data. This indicates that the dynamical stage by itself is insufficient to account for the final structural pattern in the fragment yields. The outputs of the IQMD calculations, namely the charges, mass numbers, and excitation energies of each prefragment, are then used as inputs to the GEMINI code to simulate the subsequent statistical de-excitation through sequential particle emission and binary decay. After including this secondary decay treatment, the calculated EFCSs reproduce not only the overall decreasing trend but also the phase and amplitude of the observed odd-even staggering, indicating that the odd-even effect is generated predominantly during the de-excitation of the hot prefragments rather than in the early dynamical stage, which is consistent with the findings of previous works [16, 26].

To characterize the strength of odd-even staggering in the EFCSs, the quantity $V_{oe}(\Delta Z)$ [38] is introduced as:

$$V_{oe}(\Delta Z) = \frac{2\sigma(\Delta Z)}{\sigma(\Delta Z+1)+\sigma(\Delta Z-1)}, \tag{4}$$

where $\sigma(\Delta Z)$ denotes the EFCS for a given charge change ΔZ. In Fig. 4, the $V_{oe}(\Delta Z)$ values are shown as a function of ΔZ for the EFCSs of ^{36}Ar, ^{34}Cl, ^{32}S, ^{30}P, and ^{28}Si on a carbon target. For the even-even projectiles ^{36}Ar, ^{32}S, and ^{28}Si, $V_{oe}(\Delta Z)$ exceeds 1 for even ΔZ and falls below 1 for odd ΔZ. In contrast, for the odd-odd $N = Z$ projectiles, $V_{oe}(\Delta Z)$ is larger than 1 for odd ΔZ and less than 1 for even ΔZ. This behavior is consistent with the odd-even effect, which reflects the enhanced production of even-Z fragments relative to odd-Z ones. For $\Delta Z > 2$, the $V_{oe}(\Delta Z)$ values generally approach 1 with increasing ΔZ. However, there are a few exceptions that share a common feature: $Z_P - \Delta Z = 8$; in other words, the final fragments are oxygen. One example is $V_{oe}(\Delta Z = 7)$ for ^{30}P. This can be understood from the observation in Fig. 3. Although the general trend of EFCSs suggests that $\sigma_{\Delta Z=i}$ should be higher than $\sigma_{\Delta Z=i+2}$, for ^{32}S, ^{30}P, and ^{28}Si, the EFCSs of oxygen fragments are comparable to, or even higher than, those of neon fragments, a trend that also exceeds the predictions of the IQMD+GEMINI model.

The enhancement of EFCSs for oxygen fragments has also been observed in several previous studies [5, 12–14]. Ref. [5] attributes this enhancement to the closed $Z = 8$ shell, offering a possible interpretation for the experimental observation. Moreover, similar evidence has also been observed at $Z = 14$, which is generally recognized as a closed subshell. In view of this, the underestimation of the experimental data for oxygen fragments by the IQMD+GEMINI model can be attributed to the fact that the GEMINI code provides only a phenomenological treatment of shell effects [25], which may not fully account for their influence during the de-excitation process of prefragments. However, based on the current experimental data and theoretical calculations, it remains challenging to provide a rigorous demonstration of this effect.

It is clear from Fig. 4 that the calculations by both the IQMD+GEMINI model and the FRACS empirical para-

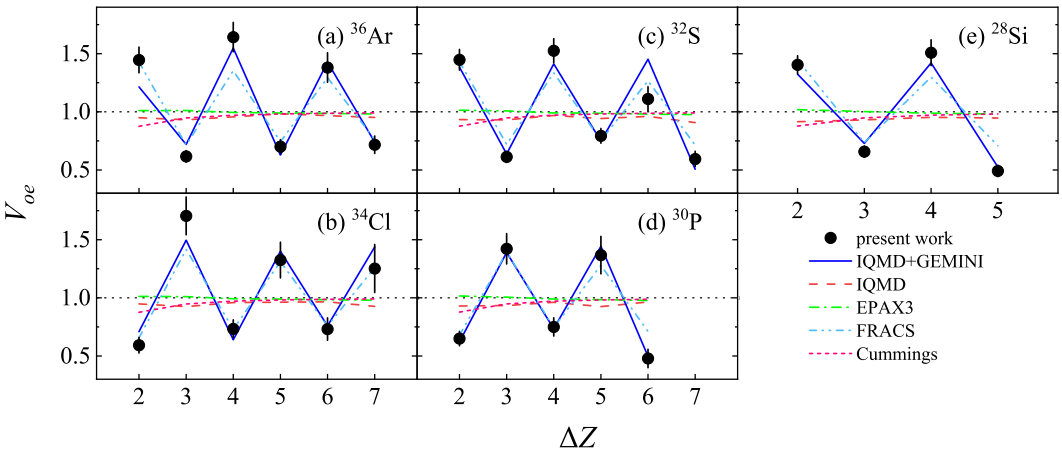

Fig. 4. (color online) Calculated odd-even staggering quantities $V_{oe}(\Delta Z)$ are shown. Experimental data are indicated by filled black circles, while model calculations are represented by various lines. The reference line at $V_{oe}(\Delta Z) = 1$ is also indicated.

metrization successfully capture the phase and most of the oscillation amplitude of $V_{oe}(\Delta Z)$. The other models, namely Cummings and EPAX3, predict an almost constant line near $V_{oe}(\Delta Z) = 1$ with no odd-even staggering.

IV. SUMMARY

In this work, we measured the EFCSs for the $N = Z$ nuclei ^{36}Ar, ^{34}Cl, ^{32}S, ^{30}P, and ^{28}Si on a carbon target at incident energies of approximately 300 MeV/nucleon. Among these, the cross sections for ^{34}Cl and ^{30}P are reported here for the first time, extending the available data along the $N = Z$ chain. The data exhibit clear odd-even staggering. A systematic comparison was made between the present results and previous measurements at similar incident energies.

The EFCSs and their associated odd-even staggering were calculated using the IQMD+GEMINI model and several empirical parametrizations. Among the various model predictions, the empirical models of Cummings and EPAX3 fail to reproduce the odd-even staggering. Both IQMD+GEMINI and FRACS reproduce well the EFCSs and the amplitude of the odd-even staggering, with IQMD+GEMINI achieving an overall accuracy of 7% in predicting the cross sections and agreeing slightly better with the experimental data than FRACS. The magnitude of the odd-even staggering decreases with increasing charge loss, with the exception of oxygen fragments. Building on earlier findings [14, 16, 26], the present results show that the odd-even staggering in EFCSs predominantly originates from the de-excitation process of excited primary fragments. Extending the analysis to the $N = Z$ chain demonstrates that this mechanism remains valid in a highly symmetric T_Z region, thereby reinforcing its robustness.

ACKNOWLEDGMENTS

We thank the HIRFL-CSR accelerator team for their efforts to provide a nice beam condition during the experiment.

References

[1] H. Geissel, P. Armbruster, K. H. Behr *et al.*, Nucl. Instrum. Meth. B **70**, 286 (1992)
[2] B. H. Sun, Chin. Sci. Bull. **65**, 3886 (2020)
[3] X. D. Xu, Y. Zheng, Z. Y. Sun *et al.*, Sci. Bull. **70**, 1026 (2025)
[4] T. Kubo, Nucl. Instrum. Meth. B **204**, 97 (2003)
[5] C. N. Knott, S. Albergo, Z. Caccia *et al.*, Phys. Rev. C **53**, 347 (1996)
[6] J. Su, F. S. Zhang, and B. A. Bian, Phys. Rev. C **83**, 014608 (2011)
[7] M. V. Ricciardi, A. V. Ignatyuk, A. Kelićand *et al.*, Nucl. Phys. A **733**, 299 (2004)
[8] J. X. Cheng, J. L. Tian, and D. H. Zhang, J. Phys. G: Nucl. Part. Phys. **42**, 015102 (2014)
[9] W. R. Webber, J. C. Kish, and D. A. Schrier, Phys. Rev. C **41**, 533 (1990)
[10] C. Zeitlin, A. Fukumura, L. Helibronn *et al.*, Phys. Rev. C **64**, 024902 (2001)
[11] C. Zeitlin, S. Guetersloh, L. Helibronn *et al.*, Phys. Rev. C **76**, 014911 (2007)
[12] C. Zeitlin, S. Guetersloh, L. Heilbronn *et al.*, Phys. Rev. C **77**, 034605 (2008)
[13] K. Sawahata, A. Ozawa, Y. Saito *et al.*, Nucl. Phys. A **961**, 142 (2017)
[14] G. S. Li, J. Su, B. H. Sun *et al.*, Phys. Rev. C **107**, 024609 (2023)
[15] S. Yamaki, T. Yamaguchi, J. Kouno *et al.*, Nucl. Instrum. Meth. B **317**, 774 (2013)
[16] X. L. Wei, G. S. Li, and J. Su, Phys. Rev. C **112**, 064604 (2025)
[17] J. R. Cummings, W. R. Binns, T. L. Garrard *et al.*, Phys. Rev. C **42**, 2530 (1990)
[18] B. S. Nilsen, C. J. Waddington, J. R. Cummings *et al.*, Phys. Rev. C **52**, 3277 (1995)
[19] K. Sümmerer, W. Brüchle, D. J. Morrissey *et al.*, Phys. Rev. C **42**, 2546 (1990)
[20] K. Sümmerer and B. Blank, Phys. Rev. C **61**, 034607 (2000)
[21] K. Sümmerer, Phys. Rev. C **86**, 014601 (2012)
[22] C. Hartnack, Z. X. Li, L. Neise *et al.*, Nucl. Phys. A **495**, 303 (1989)
[23] N. Wang, Z. X. Li, and X. Z. Wu, Phys. Rev. C **65**, 064608 (2002)
[24] H. Sorge, H. Stöcker, and W. Greiner, Nucl. Phys. A **498**, 567 (1989)
[25] R. J. Charity, M. A. McMahan, G. J. Wozniakothers *et al.*, Nucl. Phys. A **483**, 371 (1988)
[26] G.-S. Li, B. H. Sun, J. Su *et al.*, Phys. Lett. B **859**, 139143 (2024)
[27] J. W. Xia, W. L. Zhan, B. W. Wei *et al.*, Nucl. Instrum. Meth. A **488**, 11 (2002)
[28] X. Zhang, R. J. Hu, C. G. Lu *et al.*, Nucl. Phys. Rev. **34**, 290 (2017)
[29] X. H. Zhang, S. W. Tang, P. Ma *et al.*, Nucl. Instrum. Meth. A **795**, 389 (2015)
[30] J. W. Zhao and B. H. Sun, Nucl. Phys. Rev. **35**, 362 (2018)
[31] F. Fang, S. W. Tang, S. T. Wang *et al.*, Nucl. Phys. Rev. **39**, 65 (2022)
[32] J. W. Zhao, B. H. Sun, I. Tanihata *et al.*, Nucl. Instrum. Meth. A **823**, 41 (2016)
[33] W. J. Lin, J. W. Zhao, B. H. Sun *et al.*, Chin. Phys. C **41**, 066001 (2017)
[34] C. J. Wang, G. Guo, H. J. Ong *et al.*, Chin. Phys. C **47**, 084001 (2023)
[35] T. Yamaguchi, S. Fukuda, G. W. Fan *et al.*, Phys. Rev. C **82**, 014609 (2010)
[36] B. Mei, Phys. Rev. C **95**, 034608 (2017)
[37] J. Su and C. C. Guo, Phys. Rev. C **97**, 054604 (2018)
[38] G. Iancu, F. Flesch, and W. Heinrich, Radiat. Meas. **39**, 525 (2005)